Atom Indonesia

Journal homepage: http://atomindonesia.brin.go.id

Evaluation of Tumor Control Probability and Normal Tissue Complication Probability of Breast Cancer Treatment Plan in Post Mastectomy Radiation Therapy

S. Herwiningsih[1*], F. Yuana[1], R. Latifah[1], A. Hidayat[1], D. P. Rahmahtullah[1], I. Alviani[1], F. K. Hentihu[2]

[1]*Physics Departement, Faculty of Mathematics and Natural Science, Universitas Brawijaya, Jl. Veteran 1 Malang, East Java, 65145, Indonesia*
[2]*Radiotherapy Department, Lavalette Hospital, Jl. W. R. Supratman 10, Malang, East Java, 65111, Indonesia*

ARTICLE INFO

Article history:
Received 19 January 2024
Received in revised form 4 April 2024
Accepted 4 April 2024

Keywords:

Breast cancer
Normal tissue complication probability
Post mastectomy
Radiation therapy
Tumour control probability

ABSTRACT

Radiotherapy has been widely used to treat cancer, including breast cancer treatment, which can be given after patients undergo mastectomy procedures. This study aims to evaluate tumor control probability (TCP) and normal tissue complication probability (NTCP) of three-dimensional conformal radiation therapy (3DCRT) and intensity modulated radiation therapy (IMRT) treatment planning in post-mastectomy breast cancer radiation therapy. Twenty clinical breast cancer treatment plans delivered using 3DCRT were evaluated retrospectively. The IMRT plans were created for the same patients. The dose-volume histograms of each plan were extracted from the Treatment Planning System (TPS) computer which were then used to compute the TCP and NTCP for each plan. The TCP was calculated using the Poisson model and the NTCP was calculated using the Lyman-Kutcher-Burman (LKB) model. The NTCP was calculated for normal lung tissue, heart, esophagus, and spinal cord. The results show that the TCP of the 3DCRT and IMRT plans are not significantly different, with a value of above 99 %. The NTCP of the left lung is lower in the IMRT plans while the NTCP of the esophagus is lower in the 3DCRT plans. The NTCP for the heart, spinal cord, and right normal lung are zero in all plans.

INTRODUCTION

The global incidence of cancer in 2020 amounted to around 19.3 million new cases, according to the estimations provided by GLOBOCAN 2020, with a corresponding mortality rate of nearly 10 million deaths. Female breast cancer has replaced lung cancer as the most commonly diagnosed cancer, with an estimated of 2.3 million new cases (11.7 %) [1]. Breast cancer also has overtaken cervical cancer as the leading cause of cancer deaths among women (15 per 100,000) in economically developing countries [2].

The choice of breast cancer treatment is determined by factors such as the grade, stage, and molecular subtype of the disease. This approach aims to provide a treatment plan that is tailored to the individual patient, prioritizing safety and efficacy [3]. The collaboration of multi-subspecialties is vital for the diagnosis and treatment of invasive breast cancer. The use of diagnostic imaging work-up and biopsy is important in the establishment of a diagnosis, as well as in providing information for surgical decisions on management of the primary tumor, staging determination, and sequence of therapy. A significant number of women diagnosed with early-stage breast cancer are eligible for either breast-conserving surgery followed by radiation or mastectomy. There is no substantial disparity observed in the chance of local recurrence and the probability of survival between these therapies [2,4,5]. Adjuvant radiotherapy plays a key role

*Corresponding author.
E-mail address: herwin@ub.ac.id
DOI: https://doi.org/10.55981/aij.2024.1423

in the treatment of breast cancer. Following conservative surgery for an infiltrating carcinoma, radiotherapy should be systematically performed because it might reduce the rate of local recurrence, so that the occurrence of specific mortality can be prevented [6].

Radiotherapy treatment plans are assessed by evaluating the 3D dose distributions calculated by a treatment planning system (TPS). Typically, the evaluation process includes the following: (1) looking at the dose distribution superimposed on images of the patient anatomy, and (2) examining dose volume histograms (DVHs), which are 1D representations of 3D dose information for each organ or tumor volume of interest [7]. The most adopted radiation therapy treatment in breast cancer patients is 3D conformal radiation therapy (3DCRT), which has improved the outcomes of treatment [8]. With these methods of assessment, acceptance or rejection of a plan relies on an implicit estimation of the tumor control probability (TCP) and normal tissue complication probability (NTCP) arising from the dose distribution [7]. The goal of radiotherapy in breast cancer is to offer a treatment plan that results in the minimum NTCP and maximum TCP [9]. Cell biological factors, which are known as 5R radiobiology that contain repair, repopulation, reoxygenation, redistribution, and radiosensitivity can also affect the value of TCP. Meanwhile, the dose-volume effect can be represented by NTCP from the probability of complications in the irradiated organ [10]. The use of IMRT to treat whole breast cancer improves both dose homogeneity and target coverage, as well as increases the dose to normal tissue compared with 3DCRT [11]. However, as the IMRT uses a higher monitor unit (MU) compared to the 3DCRT, the treatment time becomes longer in the IMRT delivery. The selection of IMRT over the 3DCRT technique should be then evaluated not only based on physical dosimetric parameters but also considering the radiobiological parameters, expressed as TCP and NTCP.

The study aimed to evaluate the TCP and NTCP of the breast cancer treatment plan delivered using 3DCRT and IMRT techniques. Twenty post-mastectomy left-sided breast cancer plans were studied retrospectively. The radiobiological analysis was performed by using the Poisson and LKB models. The Poisson model is the most popular mathematical model used to estimate the TCP, while the LKB model is commonly used to estimate the NTCP.

MATERIALS AND METHODS

The plans used in this study were 3DCRT treatment plans for breast cancer patients treated in the Lavalette Hospital Malang from July to December 2022. Twenty treatment plans were sorted from the TPS computer with inclusion criteria of female patients and left-sided breast cancer post-mastectomy. The patients were treated using a 6 MV photon beam from the Elekta Synergy Platform linear accelerator with the dose prescription of 50 Gy in 25 fractions, 5 fractions in a week.

The IMRT plans were then created for the same patients using the Monaco TPS software ver. 5.11.03. The IMRT plans consisted of five radiation fields with the gantry angle of 330°, 300°, 30°, 110°, and 140°. The dose prescription used in the IMRT plans was the same as the 3DCRT plans, i.e., 50 Gy in 25 fractions. The objective of the treatment was to deliver 95 % of the prescribed dose to the 95 % of the PTV volume (V95 % ≥ 95 %) and the PTV volume receiving ≥ 107 % of the prescribed dose should be less than 1 % (V107% < 1 %). The dose constraint for the organ at risk (OAR) followed the QUANTEC recommendation [12] is shown in Table 1. Four OARs have been considered in the evaluation, i.e., normal lung, heart, esophagus, and spinal cord.

Table 1. Dose constraints for breast cancer radiation therapy.

Organ	Parameter	Constraint	Ref.
Normal Lung	D_{mean}	20 Gy	[13]
Heart	D_{mean}	<26 Gy	[14,15]
Esophagus	D_{mean}	<34 Gy	[16]
Spinal Cord	D_{max}	46 Gy	[17]

The dose distribution of the 3DCRT and IMRT plans were computed using the collapsed cone convolution and monte carlo algorithms, respectively, available in the Monaco TPS software. Once the dose distribution was obtained, the dose volume histograms (DVHs) were then derived from both the 3DCRT and IMRT plans. These DVHs were imported from the TPS software in csv format to be used for the calculation of TCP and NTCP in another general personal computer.

The TCP and NTCP were calculated using Biosuite software [18] in which the DVHs were used as the input for the calculation. The TCP calculation was performed using the Poisson model while the NTCP calculation was performed using the Lyman-Kutcher Burman model. These models are often used in commercial TPS software to estimate the radiobiological parameters.

The Poisson model has been used widely to estimate the TCP based on the Poisson distribution

of surviving clonogen and linear quadratic model of cell surviving curve. This model is expressed mathematically using Eq. (1).

$$TCP = \exp[-N_0 \exp(-\alpha D - \beta d D)] \quad (1)$$

Where N_0 is the number of clonogenic tumour cells per tumour volume, D is the total dose, d is the dose per fraction, α reprensents probability of irreparable damages, and β represents probability of repairable damages from irradiation.

The LKB model is commonly used to quantify normal tissue damage in which the NTCP is presented as the function of dose (D) and the irradiated volume (V). The NTCP is expressed mathematically in Eq. (2) to Eq. (4).

$$NTCP = \frac{1}{2\pi}\int_{-\infty}^{t} e^{-x^2/2} dx \quad (2)$$

$$t = \frac{D_{eff} - TD_{50}}{m.TD_{50}} \quad (3)$$

$$D_{eff} = \left(\sum_i v_i D_i^{1/n}\right)^n \quad (4)$$

where D_{eff} is the dose that gives the same NTCP for a non-uniform dose distribution as if the volume was irradiated uniformly, TD_{50} is the uniform dose that results in 50 % of complication, m is a slope of the sigmoidal dose response curve, n is a volume effect parameter, and (D_i,v_i) are the bin of a differential DVH [19].

Parameters used in the TCP calculation are shown in Table 2, and parameters used in the NTCP calculation are shown in Table 3.

Table 2. Parameters for the TCP calculation.

Parameter	Value	Ref.
Clonogen Density	1000 Cells/cm^3	[20]
Alpha	0.51 Gy^{-1}	[20]
Alpha/beta	4 Gy	[21]
Alpha spread	0.08	[21]
Repopulation constant	12	[20]
Delay before repopulation	12	[20]

Table 3. Parameters for the NTCP calculation.

OAR	m	TD50 (Gy)	n	α/β	Endpoint
Heart	0.1	48	0.35	2.5	Pericarditis [22]
Lung	0.18	24.5	0.87	4.4	Pneumonitis [20]
Spinal Cord	0.18	66.5	0.05	3.9	Myelitis/necrosis [22]
Oesophagus	0.32	51	0.44	4.9	Oesophagitis [22]

RESULTS AND DISCUSSION

The PTV coverage, which is the PTV volume receiving 95 % of the prescribed dose (V95 %), is presented in Table 4. It is shown that the IMRT plan produced a slightly higher V95 % value compared to the 3DCRT plans with a median V95 % value of 95.04 % for the 3DCRT and 96.02 % for the IMRT plans. Figure 1 shows the distribution of target coverage over twenty treatment plans for both 3DCRT and IMRT techniques. The 95 % dose prescription in all of 3DCRT plans has covered 95 % of the PTV volume. Figure 1 shows that the IMRT plans have a better target coverage than the 3DCRT plans, confirming the mean V95 % value presented in Table 4.

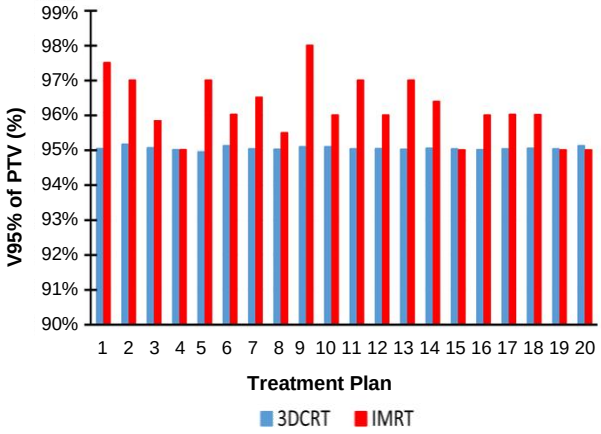

Fig. 1. The target coverage (V95 % of the PTV) for the 3DCRT and IMRT plans.

Table 4. The PTV coverage (V95 %) of the 3DCRT and IMRT plans.

Technique	Mean±sd (%)	Median (%)
3DCRT	95.05 ± 0.05	95.04
IMRT	96.27 ± 0.84	96.02

Table 5. Dosimetric parameters of the OARs from the 3DCRT and IMRT plans.

Parameter	3DCRT plan		IMRT plan	
	Mean±SD (Gy)	Median (Gy)	Mean±SD (Gy)	Median (Gy)
D_{mean} of left lung	17. 62 ± 2.16	17.77	17.72 ± 2.00	18.10
D_{mean} of right lung	0.77 ± 0.10	0.77	3.55 ± 1.11	3.37
D_{mean} of Oesophagus	7.06 ± 4.52	6.02	10.30 ± 4.80	1.02
D_{mean} of heart	9.16 ± 2.69	8.67	9.55 ± 1.50	9.80
D_{max} of spinal cord	10.59 ± 8.93	7.88	17.68 ± 6.97	17.25

Table 5 summarizes the dosimetric parameters of the OARs. The results show that the average value of D_{mean} received by

the left lung, right lung, esophagus, and heart as well as the average value of D_{max} to the spinal cord is higher in the IMRT plans compared to the 3DCRT plans. However, the value of the dose received by all OARs are still below the constraint from the QUANTEC (Table 1).

The average value of TCP and NTCP of the 3DCRT and IMRT plans are shown in Table 6. The TCP of the 3DCRT plans is slightly higher than the IMRT plans, but both of the plans have a TCP of higher than 99 %. This indicates that the designed treatment plans have a high probability of controlling the tumor. Figure 2 shows the TCP value for both the 3DCRT and IMRT plans over twenty treatment plans. Although the average value of the TCP is higher than 99 %, there is one IMRT plan that has a TCP of less than 99 % (i.e., 92 %). For this plan, the dose distribution is more homogenous in the 3DCRT plan compared to the IMRT plan as shown in Fig. 3. Although the objective V95 % has been fulfilled in plan 2, the TCP results are different.

Table 6. TCP and NTCP value of the 3DCRT and IMRT plans.

Parameters	3DCRT plan		IMRT plan	
	Mean±SD (%)	Median (%)	Mean±SD (%)	Median (%)
TCP	99.66 ± 0.40	99.80	99.57 ± 1.71	100.00
NTCP of left lung	9.02 ±6.20	7.25	5.77 ± 3.90	5.00
NTCP of oesophagus	1.47 ± 1.72	0.80	2.11 ± 1.69	1.80

On the other hand, the NTCP of the left lung is higher in the 3DCRT plans compared to the IMRT plans. The mean value of the NTCP of the left lung is 9.02 ± 6.20 % for the 3DCRT plans while for the IMRT plans the value is 5.77 ± 3.90 %. The NTCP of the left lung over twenty plans is shown in Fig. 4. Seven 3DCRT plans have an NTCP larger than 10 % while there are only four IMRT plans that have an NTCP exceeding 10 %. The NTCP to the left lung is relatively high in plan 4 and plan 16, with the highest NTCP found in plan 4 (22.9 %) delivered using 3DCRT. For this plan, the Dmean received by the left lung is the highest among other plans (i.e., 20.92 Gy). The relationship between lung D_{mean} and NTCP of lung radiation pneumonitis is shown in Fig. 5. It is shown that as the D_{mean} of the left lung increases, the probability of complication also increases exponentially.

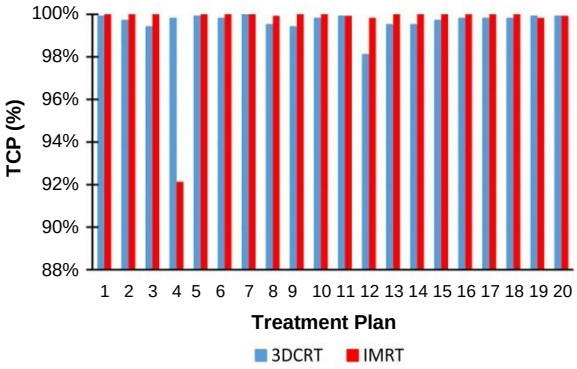

Fig. 2. The TCP value of the 3DCRT and IMRT plans.

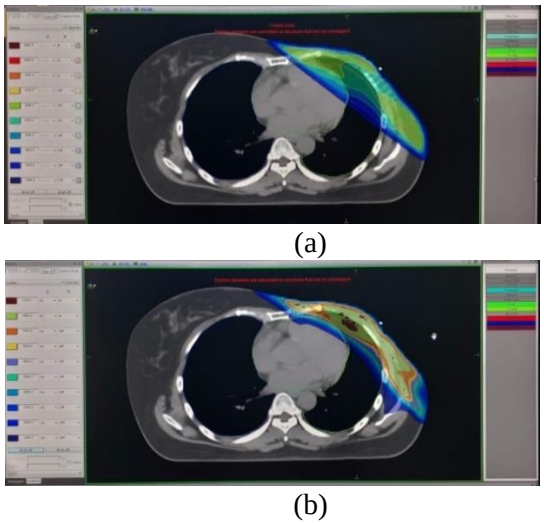

(a)

(b)

Fig. 3. The dose distribution of plan 4: a) 3DCRT plan, b) IMRT plans.

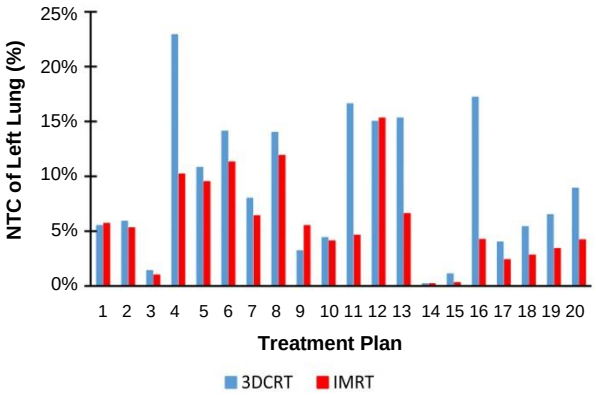

Fig. 4. The NTCP of the left lung.

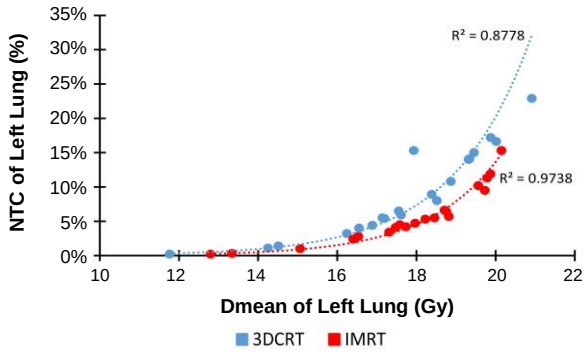

Fig. 5. The relationship between D_{mean} of left lung and NTCP.

The IMRT plans show a higher NTCP value for the esophagus with a mean value of 2.11 ± 1.69 % compared to the 3DCRT with the mean value of 1.47 ± 1.72 %. Since the NTCP of the esophagus is less than 5 %, it is expected that the probability of complication to the esophagus is minimal. The NTCP for other OARs, i.e., right lung, heart, and spinal cord were zero for all plans, indicating low complication probabilities for these organs.

The IMRT technique has been claimed to offer better OAR sparing compared to the 3DCRT technique. The study of skin dose comparison between 3DCRT and IMRT techniques in post-mastectomy breast radiation therapy by Hentihu et al. [23] shows that the IMRT technique reduces the dose received by the skin compared to the 3DCRT plans. Another study by Adeneye et al. [24] shows that the IMRT has a superior homogeneity and high-dose volume sparing to OAR compared to the 3DCRT. However, in this study, we found that the IMRT technique results in almost similar dosimetric parameters to OARs even resulting in a higher dose to the esophagus and spinal cord compared to the 3DCRT technique.

The superiority of the IMRT is shown in the target coverage of the PTV and the NTCP of the left lung. However, there is no significant difference in the TCP value obtained from those two techniques. Wang et al. [25] reported that in right-sided breast cancer radiotherapy, the TCP and NTCP of the right lung are not significantly different between 3DCRT, four-field IMRT, and single arc VMAT techniques. They found that IMRT results in a better target coverage compared to other techniques, which is similar to the finding obtained from our study. Similar results are reported by Shanei et al. [11] that there is no significant difference in the TCP value obtained from 3DCRT, six-field IMRT and nine-field IMRT.

The superiority of the IMRT in dosimetric parameter to the PTV is also reported by Liu et al. [26]. However, as the IMRT technique requires a higher MU, it has a consequence of increasing treatment time which is unsuitable in a busy radiotherapy department. This limitation of IMRT makes VMAT a good alternative technique since VMAT offers a shorter treatment time and a lower MU. However, the implementation of VMAT is still limited to certain hospitals as it requires a more advanced linac machine. Another alternative to 3DCRT and IMRT technique in breast cancer radiotherapy is hybrid IMRT. A study by Bi et al. [27] shows that hybrid IMRT achieves a better target quality and OAR sparing in simultaneous integrated boost radiotherapy for right-side breast cancer compared to IMRT and hybrid VMAT techniques.

CONCLUSION

This study has evaluated the TCP and NTCP values of post-mastectomy breast cancer treatment plans delivered using 3DCRT and IMRT techniques. The 3DCRT plans produce a slightly higher TCP plan compared to the IMRT plans, but both techniques produce a TCP of higher than 99 %, indicating a high probability of controlling the tumors. Although the average value of the mean dose received by the organ-at-risks are higher in the IMRT plans, but the NTCP for several OARs was zero, and only the NTCP of the left lung needs a higher concern, especially in the 3DCRT plans. Overall, the IMRT plans result in a smaller complication probability on the normal left lung compared to the 3DCRT plans while having a similar probability of controlling the tumor. The NTCP for the heart, spinal cord, and right normal lung are zero in all plans.

ACKNOWLEDGMENT

The authors would like to thank all those who have supported the completion of this research. The authors would also like to thank the Faculty of Mathematics and Natural Sciences, Universitas Brawijaya for funding this research.

AUTHOR CONTRIBUTION

All authors equally contributed as the main contributors of this paper. All authors read and approved the final version of the paper.

REFERENCES

1. H. Sung, J. Ferlay, R.L. Siegel *et al.*, CA Cancer J. Clin. **71** (2021) 209.
2. X. Yang, C. Zhu and Y. Gu, PLoS One **10** (2015) e0125655.
3. A. Burguin, C. Diorio and F. Durocher, J. Pers. Med. **11** (2021) 808.
4. T. A. Moo, R. Sanford, C. Dang *et al.*, PET Clin. **13** (2018) 339.
5. I. Ratosa, G. Plavc, N. Pislar *et al.*, Cancers **13** (2021) 4044.
6. C. Hennequin, Y. Belkacémi, C. Bourgier *et al.*, Cancer/Radiothérapie **26** (2022) 221.

7. B. Warkentin, P. Stavrev, N. Stavreva *et al.*, J. Appl. Clin. Med. Phys. **5** (2004) 50.
8. Yim, C. Suttie, R. Bromley *et al.*, J. Med. Radiat. Sci. **62** (2015) 184.
9. S. Herwiningsih, A. Naba, S. Rianto *et al.*, Indonesian Physical Review **6** (2023) 284.
10. D. N. Teguh, R. B. Raap, H. Struikmans *et al.*, Radiat. Oncol. **11** (2016) 130.
11. A. Shanei, A. Amouheidari, I. Abedi *et al.*, Int. J. Radiat. Res. **18** (2020) 315.
12. S. M. Bentzen, L. S. Constine, J. O. Deasy *et al.*, Int. J. Radiat. Oncol. Biol. Phys. **76** (2010) S3.
13. L. B. Marks, S. M. Bentzen, J. O. Deasy *et al.*, Int. J. Radiat. Oncol. Biol. Phys. **76** (2010) S70.
14. G. Gagliardi, L. S. Constine, V. Moiseenko *et al.*, Int. J. Radiat. Oncol. Biol. Phys. **76** (2010) S77.
15. X. Wei, H. H. Liu, S. L. Tucker *et al.*, Int. J. Radiat. Oncol. Biol. Phys. **70** (2008) 707.
16. M. Werner-Wasik, E. Yorke, J. Deasy *et al.*, Int. J. Radiat. Oncol. Biol. Phys. **76** (2010) S86.
17. J. P. Kirkpatrick, A. J. Van Der Kogel, and T. E. Schultheiss, Int. J. Radiat. Oncol. Biol. Phys. **76** (2010) S42.
18. Uzan and A. E. Nahum, Br. J. Radiol. **85** (2012) 1279.
19. Herwiningsih, Dosimetric Verification of Stereotactic Body Radiotherapy Treatment Plans for Early Stage Non-Small Cell Lung Cancer Using Monte Carlo Simulation, Ph.D. Thesis, Queensland University of Technology (2017).
20. K. S. T. Abi, S. Habibian, M. Salimi *et al.*, Arch. Breast Cancer **8** (2021) 192.
21. X. S. Qi, J. White, X. A. Li, Radiother. Oncol. **100** (2011) 282.
22. J. H. Chang, C. Gehrke, R. Prabhakar *et al.*, Physica Med. **32** (2016) 248.
23. F. K. Hentihu, A. K. Anto and R. S. Nugroho, Atom Indones. **48** (2022) 9.
24. S. Adeneye, M. Akpochafor, B. Adegboyega *et al.*, Eur. J. Breast Health **17** (2021) 247.
25. J. Wang, X. Li, Q. Deng *et al*., Med. Dosim. **40** (2015) 190.
26. H. Liu, X. Chen, Z. He *et al.*, Comput. Med. Imaging Graphics **54** (2016) 1.
27. S. Bi, R. Zhu and Z. Dai, Radiat. Oncol. **17** (2022) 60.